J. Fluid Mech. (2007), *vol.* 585, *pp.* 41–71.
doi:10.1017/S0022112007006490 Printed in the United Kingdom

Reactive control of transition induced by free-stream turbulence: an experimental demonstration

FREDRIK LUNDELL

Linné Flow Center, KTH Mechanics, Royal Institute of Technology, S-100 44, Stockholm, Sweden

(Received 9 March 2005 and in revised form 10 January 2007)

The present wind-tunnel experiment demonstrates that a reactive control system is able to decrease the amplitude of random disturbances in a flat-plate boundary layer. The disturbances were induced in a laminar boundary layer by a turbulent free stream. The control system consisted of upstream wall-shear-stress sensors (wall wires) and downstream actuators (suction through holes). An *ad hoc* threshold-and-delay control algorithm is evaluated and parameter variations were performed in order to find a suitable working point of the control system. Detailed measurements of the flow field show how the control influences the disturbances in the boundary layer, whereas the effect on the mean flow owing to the control is minute. The control system manages to inhibit the growth of the fluctuations of the streamwise velocity component for a considerable distance downstream of the two actuator positions. Further downstream, however, the amplitudes of the fluctuations grow again. The flow rate used to obtain the control effect is one sixth of that necessary if continuous distributed suction is used to reach the same control objective. Finally, correlations and spectra show that the elongation of the structures in the streamwise direction is eliminated in the regions where the control has the largest effect. The spanwise scale of the disturbances is not affected by the control.

1. Introduction

In this work, a reactive control system has been used to decrease disturbance growth in a boundary layer subjected to free-stream turbulence (FST). The possibilities of dynamic control of turbulence and transition have been demonstrated numerically by a vast number of studies; however, the schemes are often impossible to implement in physical set-ups. The present work has two goals. The first is to determine to what extent available technology can be used for experimental flow control studies and the second is to elucidate how the disturbances in the flow are affected by the control. The control system which is used in the present study is the simplest possible after continuous distributed suction, and the present results could also serve as a benchmark to aim at for future studies.

Transition induced by free-stream turbulence was chosen as a model case for two main reasons. First, the route to turbulence of a laminar boundary layer subjected to free-stream turbulence above about 1 % is well documented: an initial growth of high- and low-speed streaks followed by high-frequency oscillation and eventually the formation of turbulent spots, resembling the self-generation cycle of turbulence. Secondly, the length and time scales are much larger than in comparable fully turbulent cases, which simplifies the construction of the control apparatus. This

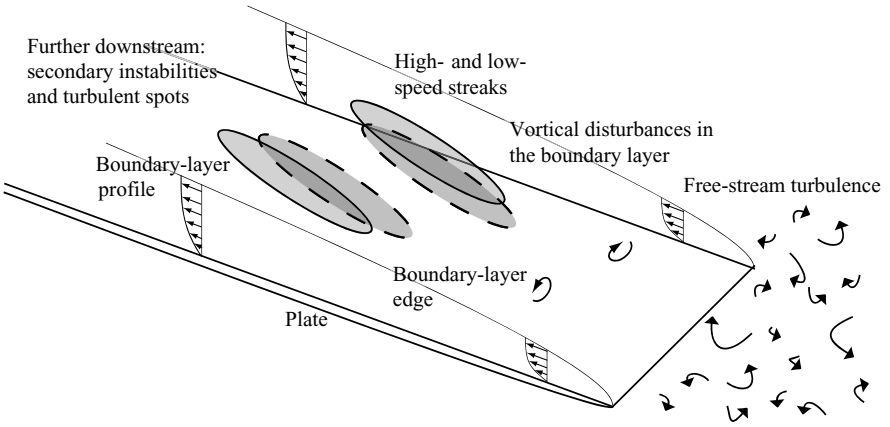

FIGURE 1. Sketch of the disturbances in and around a boundary layer subjected to free-stream turbulence. The free-stream turbulence forces vortical motions in the boundary layer which interact with the mean velocity gradient and generate streaks of low (dashed) and high (solid) velocity. The low-speed streaks are correlated with upward motions and the high-speed streaks with downward motions.

introduction continues with reviews of the recent development of FST induced transition and flow control.

1.1. *Streaks and their breakdown*

Prior to the breakdown to turbulence of a laminar boundary layer subjected to free-stream turbulence, velocity streaks are observed if the turbulence intensity is above about 1 % (figure 1) (Kendall 1998). Matsubara & Alfredsson (2001) and Lundell & Alfredsson (2004) studied the development of these structures in detail. In the zero-pressure-gradient boundary layers usually studied, the root-mean-square (r.m.s.) value of the streamwise velocity is often seen to grow in linear proportion to the boundary-layer thickness. The spanwise scale of the disturbances is of the order of the boundary-layer thickness and the structures are increasing in streamwise length as they propagate downstream. The streaks are known to be generated by the so called lift-up effect (Landahl 1980) since wall-normal velocity disturbances lift low-velocity fluid from close to the wall to higher regions in the boundary layer. The action of lift-up has been verified both numerically and experimentally (Jacobs & Durbin 2001; Inasawa *et al.* 2003).

The primary disturbances, the streaks, give rise to r.m.s.-amplitudes of 10–15 % prior to breakdown (Matsubara & Alfredsson 2001). The wall-normal profile of u_{rms} has its maximum at approximately half the boundary-layer thickness away from the wall and agrees well both with the distribution obtained by Leib, Wundrow & Goldstein (1999) with asymptotic expansions and with optimal disturbance theory by Andersson, Berggren & Henningson (1999) and Luchini (2000). The optimal disturbance theory shows that linear mechanisms can act as amplifiers of disturbances in the boundary layer. However, it does not explain (*i*) that the disturbance level in the free stream is finite, (*ii*) that the free stream forces the boundary layer continuously, and (*iii*) how the disturbances are introduced into the boundary layer. These limitations are, of course, of utmost importance when modelling the physical process.

These issues are discussed by Wundrow & Goldstein (2001) and efforts have been (and are being) made to construct more complete theoretical frameworks (e.g.

asymptotic expansions) in which these issues are accounted for (Leib *et al.* 1999; Wundrow & Goldstein 2001; Ricco *et al.* 2004). The results show both that the continuous forcing of the free stream has an effect on the growth and that nonlinear effects result in interactions between the free stream and the boundary layer. A dependence on the length scales and isotropy of the free-stream turbulence is also found in these studies. It has also been concluded that the spanwise component of the free-stream fluctuations are the most important for the generation of high-amplitude disturbances in the boundary layer.

Experiments performed by Jonáš, Mazur & Uruba (2000) show that if the spacing of the turbulent generating grid is large enough (and, as a result, the turbulence decays sufficiently slowly), the amplitude growth of disturbances in the boundary layer is independent of the turbulent scales in the free stream. A complete theory of this puzzling phenomenon is yet to be established.

Direct numerical simulations (DNSs) of the streak growth and breakdown process have been performed (Jacobs & Durbin 2001). The DNS studies confirm most of the experimental findings and add a considerable amount of information on how various scales in the free stream penetrate down into the boundary layer.

The later stages of breakdown might be due to secondary instabilities of the streaks, as proposed by e.g. Matsubara & Alfredsson (2001) and studied experimentally by Elofsson, Kawakami & Alfredsson (1999) and Asai, Minagawa & Nishioka (2002). Theoretical analysis of the secondary instability of streaks can be found in Reddy *et al.* (1998), Andersson, Brandt & Henningson (2001) and Hœppner, Brandt & Henningson (2005). It has been found that if the streak amplitude is large enough, secondary instabilities will be amplified (exponentially or transiently) by the streak. Alternatives to the secondary instability scenario have been suggested. Two candidates are growth of two-dimensional waves (Bakchinov *et al.* 1995; Fasel 2002) and interaction between the streaks and small scales in the free stream as suggested by Jacobs & Durbin (2001). These standpoints are somewhat unified by Zaki & Durbin (2006) who first showed that coupling coefficients can be used to quantify how different eigenmodes in the free stream can generate disturbances in the boundary layer. Zaki & Durbin (2006) then demonstrate (in a DNS) that the full transition scenario can be regenerated if the flow is forced with one strongly coupled low-frequency mode (generating streaks) and one weakly coupled high-frequency mode (which forces exponentially growing secondary instabilities to appear owing to inflectional velocity profiles).

The breakdown scenario shows a strong resemblance to the regeneration cycle (transient growth of streaks, secondary instability and nonlinearity eventually leading to new streaks) of turbulence proposed by e.g. Waleffe (1995) and detected in a database from a DNS by Hamilton, Kim & Waleffe (1995). As pointed out by Wundrow & Goldstein (2001), there are differences and open questions regarding these similarities, since streaks in turbulent boundary layers are driven by disturbances already in the boundary layer whereas the streaks induced by FST are driven by external disturbances.

1.2. *Streak control*

Successful control of transition and/or turbulence would lead to large energy savings in a vast number of applications such as commercial aircrafts and pipelines. The studies reviewed below help to set the present work in its proper context. This study is an attempt to start overcoming the differences between (*a*) numerical studies in which all information is available and any type of action can be performed, and (*b*) physical experiments, where sensing and actuation can be performed at a limited

number of discrete locations. In air, there is also an additional restriction, namely that the actuation must be done at the wall. In conducting fluids, e.g. salt water, electrodynamic forces acting away from the wall can be used for the actuation.

1.2.1. *Numerical studies on control of transition and turbulence*

Streaks are a vital ingredient both in transition induced by free-stream turbulence and in the turbulence regeneration cycle. It could therefore be expected that control of FST-induced transition has similarities with control of turbulence. The idea behind control of turbulence in this context, is that a minute energy input can change the flow dynamics drastically, so that the friction drag generated by the turbulence at a wall is decreased. In practice, this can be achieved by varying the wall-normal velocities at the walls according to some control law. Below, some of the major studies in this field are reviewed.

In a DNS, Choi, Moin & Kim (1994) showed that the skin friction in a turbulent channel flow can be reduced by a control scheme named *opposition control*. In opposition control, the wall-normal velocity at a certain distance from the wall is measured and the velocity at the wall is prescribed to be the same but with opposite sign. The control seems to suppress streamwise vortices which would otherwise generate streaks. Thereby, the production of turbulence is decreased.

A large eddy simulation (LES) study (Chang, Collis & Ramakrishnan 2002) showed that the opposition control scheme relaminarizes turbulent channel flows at low Reynolds numbers (the Reynolds number can be defined as $Re = U_{CL}h/\nu$ where U_{CL} is the centreline velocity, h is half the channel height and ν is the kinematic viscosity of the fluid). At higher Reynolds numbers, the skin friction was reduced, but the flow remained turbulent. The reduction in turbulent skin friction decreased as the Reynolds number was increased further.

A more advanced method for determining the control input was used by Bewley, Moin & Temam (2001). They minimized the velocity fluctuations in a turbulent channel flow by direct optimization. At each time step, the local wall-normal velocities at the walls were set to values minimizing future flow oscillations. In order to achieve this, an optimization procedure returning the present optimal wall velocities had to be made at each time step. The scheme was shown to relaminarize the flow at higher Reynolds numbers than in Chang *et al.* (2002). The method is time consuming and impossible to implement in a physical experiment because of the sensing, actuation and computational demands. The results nevertheless show the possibilities of actuation at the wall.

A final example of a numerical flow-control study is the work of Högberg & Henningson (2002), who applied controllers designed by optimal control theory to transition in spatially developing boundary layers. The optimal controllers were found to decrease the fluctuation energy of single-mode disturbances very well (of the order of 10 or more), but they work less well on transiently growing multi-mode disturbances (e.g. optimal disturbances), which were reduced only at the streamwise positions at which control was applied. Downstream of the region in which control was applied, the disturbance amplitude increased again.

The numerical studies show that properly applied control has large effects on the flow and can decrease the friction drag. The control laws have seen an impressive development during the last decade. However, none of the studies mentioned above take experimental limitations into account. In an experiment, it is difficult (if not impossible) to perform sensing and actuation at the same position, actuators must have a finite size and the control action has to be calculated in real-time.

Endo, Kasagi & Suzuki (2000) performed simulations in which they imposed such limitations on the opposite control scheme of Choi *et al.* (1994). The results of Endo *et al.* (2000) show that the physical constraints reduce the efficiency of the control. It can therefore be assumed that the most impressive results from numerical studies will never be reached on experimental set-ups. Smaller, but still significant, savings can be expected.

1.2.2. *Experimental flow control*

An experimentalist who wants to study flow control neither has access to the measurements (flow-field information) available in a DNS nor the ability to perform amplitude-modulated fine-scale actuation. An additional complication when reviewing experimental studies of flow control is that it is usually not straightforward to compare results from different experiments since it is hard to determine accurate values of relevant performance measures, such as the skin friction.

The traditional aim is therefore not to study the performance of different control laws, but rather to study the effect of various types of actuation. One way to study flow control is to generate disturbances in a controlled manner, and then try to cancel them with some suitable actuation. Two examples are the studies of Gad-el-Hak (1989) and Bakchinov *et al.* (1999), who used suction through holes to inhibit the growth and breakdown of streak-like disturbances in laminar boundary layers. An alternative is to adapt the method used by Rebbeck & Choi (2001), where an actuator was activated continuously at the wall in a turbulent boundary layer. By monitoring the incoming flow, Rebbeck & Choi (2001) could use conditional averaging in the post-processing of the data to study the effect of the control on the mean disturbance in the boundary layer.

Physical realizations of complete feed-back control systems are rare. Rathnasingham & Breuer (2003) used skin friction measurements and pulsating jets to control a turbulent boundary layer. Finite impulse response (FIR) filters were used to determine (*i*) the disturbance development from the sensor to some point downstream of the actuator, and (*ii*) how the actuator influenced the flow at the same position. The control system decreased the bursting frequency and velocity fluctuations downstream of the actuator and some skin friction reduction was reported. The skin friction was, however, estimated from the mean velocity profiles, a method which is unreliable in an experiment for two main reasons. (*i*) The exact position of the wall is hard to determine with high accuracy. (*ii*) The control action might change the physics of the turbulence in the boundary layer so that the assumptions used when determining the skin friction are not valid. Historically, estimations of the skin friction based on velocity profile measurements have given misleading results when used to estimate the effect of large eddy breakup devices (LEBUS). Sahlin, Johansson & Alfredsson (1988) used direct drag mesasurements to establish that there was no net-effect of LEBUS on the total drag, in contrast to previous studies which relied on estimations based on velocity profiles.

Jacobson & Reynolds (1998) used a flap-and-cavity vortex generator to control streamwise streaks. Randomly generated disturbances in a laminar flow were controlled by two controllers: an *ad hoc* linear controller and a neural network. They showed that such a control scheme could decrease the amplitude of the disturbances.

The coupling between streak attenuation and transition delay was demonstrated by Lundell & Alfredsson (2003). They studied transition induced by secondary instabilities acting on streaks in a plane channel. The disturbances were generated artificially in a random manner. Occurrences of streaks were detected with wall wires,

and further downstream, the flow was controlled by localized suction turned on and off depending on the detection. It was demonstrated that reactively controlled localized suction could decrease the amplitude of the streaks, which in turn led to a slower growth of the secondary disturbances. Thanks to the slower growth of the secondary disturbances, the transition point was moved downstream when applying the control.

In the present experiment, intermittent suction through holes triggered by wall-wire signals from upstream sensors was used. The same concept was used by Kerho *et al.* (2000), who used in total 25 sensors and actuators and tried the system in a turbulent boundary layer. The fluctuations of the streamwise velocity component were found to decrease because of the control, and large drag reduction was reported, again based on the mean velocity profiles. Flow visualizations indicate that the control system removes the fluid of the low-velocity streaks completely, rather than performing the minute modifications of the flow aimed for in the present study.

1.3. *Present work*

The set-up, control system and controller are described in § 2. The results are presented in §§ 3–6. Section 3 presents results on velocity statistics and disturbance growth in the boundary layer. Section 4 continues with a study of how the performance of the control systems depends on the controller parameters. Further details of the effects of the control are given in §§ 5 and 6, where correlations and spectral information of the velocity and shear stress variations are studied. The results are discussed in § 7 and the conclusions are summarized in § 8.

2. Experimental set-up

2.1. *Flat-plate set-up*

The experiments were performed in the MTL wind-tunnel at KTH Mechanics in Stockholm. Details on the wind tunnel and its flow quality are reported in Lindgren (2003). The experimental set-up with turbulence generating grid, flat plate, traverse system and control system is sketched in figure 2. The flat plate was first used by Klingmann *et al.* (1993) and the leading edge is designed so that the pressure gradient on the upper side is minimized. The plate flap was adjusted so that no turbulent spots, generated by laminar separation on the upper side of the leading edge, occurred in the boundary layer. After proper flow around the leading edge had been obtained by adjusting the flap, the position of the wind-tunnel roof was adjusted in order to achieve a constant free-stream velocity along the plate. The free-stream velocity (U_∞) was 4.8 m s^{-1} ± 1 % along the plate during the measurements.

The coordinates are x, y and z for the streamwise, wall-normal and spanwise directions, respectively. The leading edge is at $x = 0$, $y = 0$. The two coordinates x and z are measured in mm while the wall-normal coordinate y is non-dimensionalized as

$$y = \frac{y^*}{\delta}, \tag{2.1}$$

where y^* is the dimensional coordinate and $\delta = (\nu x/U_\infty)^{0.5}$ where ν is the kinematic viscosity. The streamwise velocity is denoted by U where capital letters denote the mean value and lower case the fluctuations. Velocities are normalized with the free-stream velocity, U_∞.

The free-stream turbulence was generated by grids placed 1600 mm upstream of the leading edge. Two different levels of FST have been used. Grids A and B of

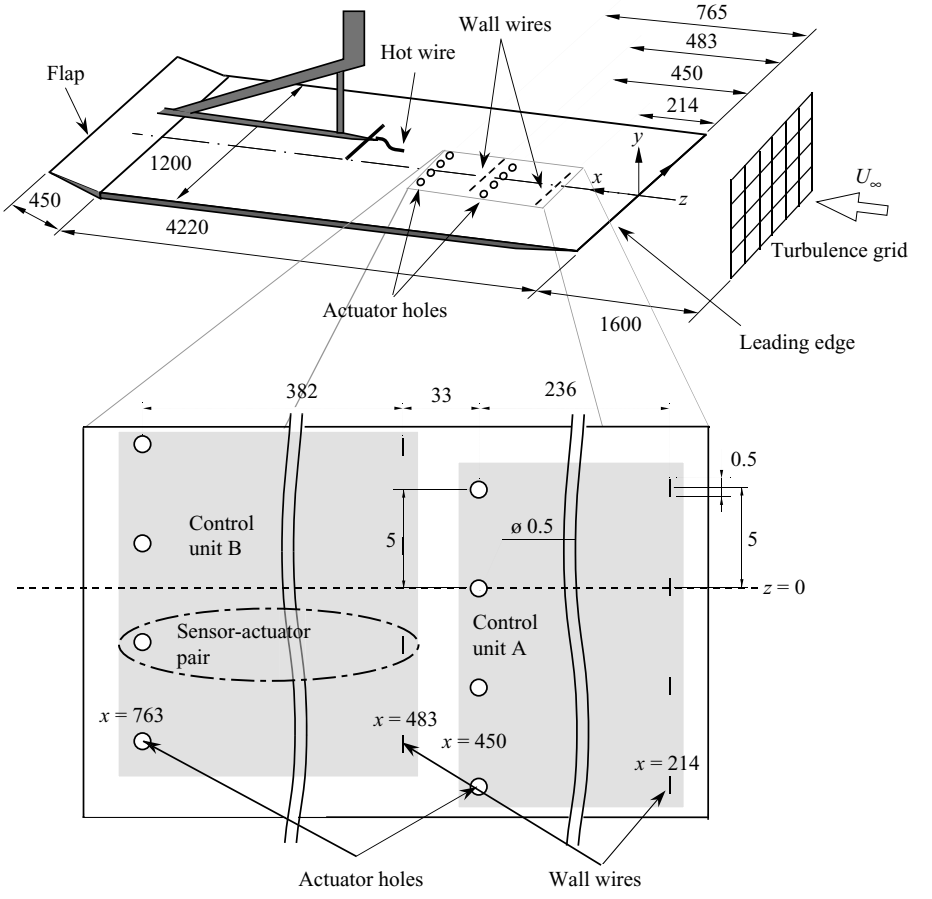

FIGURE 2. Flat-plate set-up used in the present experiment and detail of the control units. Measures are in mm.

Matsubara & Alfredsson (2001) and Fransson & Alfredsson (2003) were used. The turbulence intensity, Tu, defined as

$$Tu = \frac{u_{rms}}{U_\infty} \tag{2.2}$$

in the free stream above the leading edge was 1.4 % and 2.5 % with grids B and A, respectively.

The velocity was measured by a hot wire mounted to a three-dimensional traverse. Platinum wires with a length of 0.5 mm and a diameter of 2.5 μm were used. The hot wire was calibrated in the free stream against a Prandtl tube with no turbulence-generating grid present. It was recalibrated when the free-stream velocity measured by the Prandtl tube and the wire differed by more than 2 %. The time between calibrations varied from 2 to 11 days.

The wall position was determined by fitting velocity profiles to the theoretical Blasius solution. The velocity profiles used for this purpose were measured without turbulence-generating grids.

		(mm)	δ	ℓ^+
Unit A	Sensor width	0.5	0.60	5.6
	Separation	5.0	6.0	56
	Actuator width	0.5	0.41	4.6
	Separation	5.0	4.1	46
Unit B	Sensor width	0.5	0.40	4.5
	Separation	5.0	4.0	45
	Actuator width	0.5	0.32	4.0
	Separation	5.0	3.2	40

TABLE 1. Width and separation of the sensors and actuators in the units mm, δ and ℓ^+ (the local boundary layer and friction length scale of the Blasius boundary layer, respectively).

The velocity was sampled and digitized with 2 kHz and the sampling period was 60 s for all measurements. The hot wire was sampled together with the wall-wire signals used in the controller.

2.2. *Control system*

The control system consists of two sets, units A and B, with four sensor–actuator pairs each. The sensors were wall wires and the actuators were holes, through which suction could be turned on and off by fast solenoid valves. The suction was established by an air pump connected to a low-pressure chamber. The low-pressure chamber was large enough to cancel the fluctuations from the pump (this was checked by placing the hot wire over the entrance of the suction hole). The suction holes were positioned straight downstream of the wall wires (see figure 2). The streamwise positions of the sensors and actuators were chosen in a two-stage process. First, the approximate positions were chosen so that suitable delay times (based on the free-stream velocity) from sensor to actuator were obtained. The exact positions were then decided by where the instruments could be mounted in the plate. The positions of the two sets of sensors and actuators are given in figure 2 and the dimensions in relevant boundary-layer length-scales (δ defined above and the friction length scale, $\ell^+ = \nu(\rho/\tau_w)^{0.5}$ where ρ is the density of the air and τ_w is the friction at the wall given by the Blasius solution) are given in table 1.

The wall wires were also 0.5 mm long platinum wires with a diameter of 2.5 μm and were welded to the tip of the prongs which were flush with the wall. The wires were bent out from the wall during the welding, so that the centre of the platinum wire was positioned 25–50 μm above the wall. The wall wires were aligned in the spanwise direction in order to give a measure of the streamwise shear-stress variations. It could be argued that the spanwise shear-stress fluctuation is a better indicator of streaks. It is, however, extremely difficult to capture the spanwise shear-stress fluctuations with wall wires, since the much larger streamwise fluctuations tend to dominate even if the wires are aligned in the streamwise direction. The spanwise orientation of the wall wires was thus chosen in order to base the control on a signal with a well-defined physical origin.

2.3. *Controller*

For the control logic, the raw signal from the wall wire, E_{ww}, was normalized according to

$$W(t) = \frac{E_{ww}(t) - \overline{E_{ww}}}{E_{ww,rms}}, \tag{2.3}$$

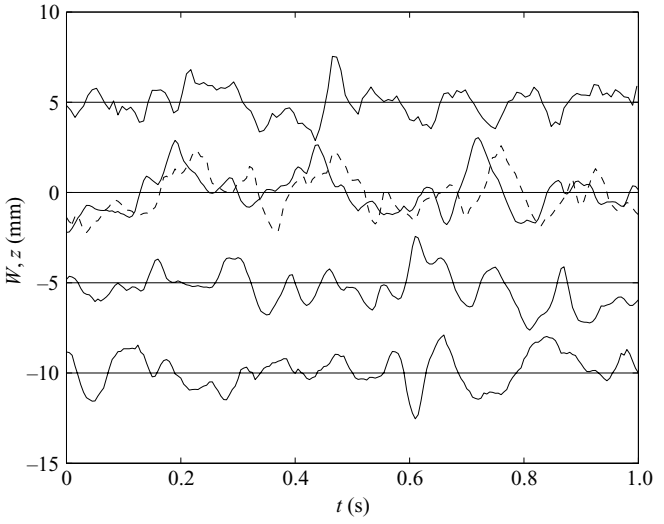

FIGURE 3. Simultaneous signals from the wall wires (W) at $x = 214$ mm, $z = -5$, 0, 5, 10 mm (solid line) and the simultaneous velocity measured by the hot wire at $x = 400$ mm, $y = 2.1$, $z = 0$ (dashed line around $z = 0$). The velocity signal has been transformed and scaled as W (see (2.3)) and the signals are separated so that they fluctuate around the value corresponding to their z-position.

where $\overline{E_{ww}}$ is the temporal mean of the raw signal from the anemometer. After this normalization, $W(t)$ is a good approximation of the (normalized) fluctuations of the wall-shear stress.

In figure 3, simultaneous time traces of the signals from the wall wires (positioned at $x = 214$ mm) and the hot-wire signal from $x = 400$ mm, $y = 2.1$, (dashed line) are shown. The velocity signal and the wall-wire signal at the same spanwise position are correlated with a time delay: a period of low shear stress at $(x, y, z) = (214\text{ mm}, 0, 0)$ (solid curve) is soon followed by a period of low velocity at $(x, y, z) = (400\text{ mm}, 2.1, 0)$ (dashed curve), showing the convective nature of the disturbances. The maximum correlation between the signals at $z = 0$ is 86 % with a delay of 34 ms. All the wall-wire signals show similar low-frequency variations. The correlations between the wall-wire signals are between -10 and 0 % for a separation of 5 mm and around -20 % with 10 mm separation. It can thus be concluded that the disturbances appearing at one sensor have no correlation to the disturbances appearing at the next sensor and there is a fairly strong negative correlation with the second sensor. This shows that most disturbances will be detected by the sensors even though there is a limited possibility that disturbances occur between two sensors.

A sensor and the actuator straight downstream of it are working independently of the other sensor–actuator pairs. The control scheme is such that the control suction was turned on with a preset delay d_c if the normalized wall-wire signal W_i upstream of sensor i was below (or above in some parameter variation tests) a preset threshold value, k. The physical rationale for the control scheme is that a low value of the shear stress indicates a streak of low velocity passing above the sensor. After a time delay, this streak has been convected to the suction holes, where the suction through the narrow hole generates vertical velocities towards the wall, which redistribute the momentum so that the streak amplitude growth decreases.

The numerical values of d_c and k could be set independently for units A and B. In the presentation of the results to follow, k is not given explicitly, instead the resulting time fraction during which control is turned on:

$$\Gamma_{on} = \frac{T_{on}}{T_{total}} \tag{2.4}$$

is used. In (2.4), T_{on} is the total amount of time the control suction is turned on during the time period T_{total} that the control system is turned on. The amplitude of the control action is measured by the mean suction velocity through the suction hole when the suction is turned on, and is denoted by V_w.

The controller was implemented in LabView and was run on an independent desktop computer at 1 kHz.

3. Velocity statistics and disturbance growth

Data from two set of experiments will be presented. The first set is taken at $Tu = 1.4\,\%$, a turbulence level at which transition does not occur within the measured region. At $Tu = 1.4\,\%$, control unit A was used. The second set of data is taken at $Tu = 2.5\,\%$ and the data includes results where both control units are used. In all cases where measurements with and without control are compared, the measurements were performed in sequence within 16 h without opening the wind tunnel in between. The accuracy of the data has been determined with the method proposed by Lumley (1970) and all mean values have an expected accuracy of better than 1 %. The r.m.s. values all have an accuracy better than 5 % where 5 % is an extreme value found close to the free stream. The major portion of the r.m.s. data has an accuracy of 3 % or lower. The parameter values of the controller are stated in § 4.4.

3.1. $Tu = 1.4\,\%$

First, the mean and disturbance structure of the basic flow, i.e. a boundary layer subjected to FST, will be presented. This is followed by the response of the mean flow to the control. The key boundary-layer data without control are summarized with circles in figure 4(*a–c*). Velocity profiles measured by the hot wire at various streamwise positions ranging from $x = 200$ to 1600 mm are compared with the theoretical Blasius solution (solid line) in figure 4(*a*) and agree well with the laminar profile. The shape factor (the quotient between the displacement and momentum thicknesses) is 2.59 ± 0.06 for all x (2.59 is the value for the Blasius velocity profile). The agreement between the velocity profiles and the theoretical undisturbed solution indicates that the disturbance growth is governed by linear mechanisms (Wundrow & Goldstein 2001).

The disturbance evolution is shown as the u_{rms} profiles in figure 4(*b*). The u_{rms} profile without control is in good agreement with the data of Kendall (1998): there is a maximum around $y = 2.1$. In the upper parts of the boundary layer, the disturbance approaches the free-stream turbulence level, which is decreasing in the downstream direction. The disturbance profiles agree well both with the analysis of Leib *et al.* (1999) and (inside the boundary layer) with the optimal growth theory (not shown) of Andersson *et al.* (1999) and Luchini (2000). At this point, it is important to remember that the latter analysis cannot predict the streamwise growth of disturbances in a continuously forced boundary layer, whereas the former allows studies of how different aspects of the free-stream disturbance (such as anisotropy) affect the growth of disturbances in the free stream.

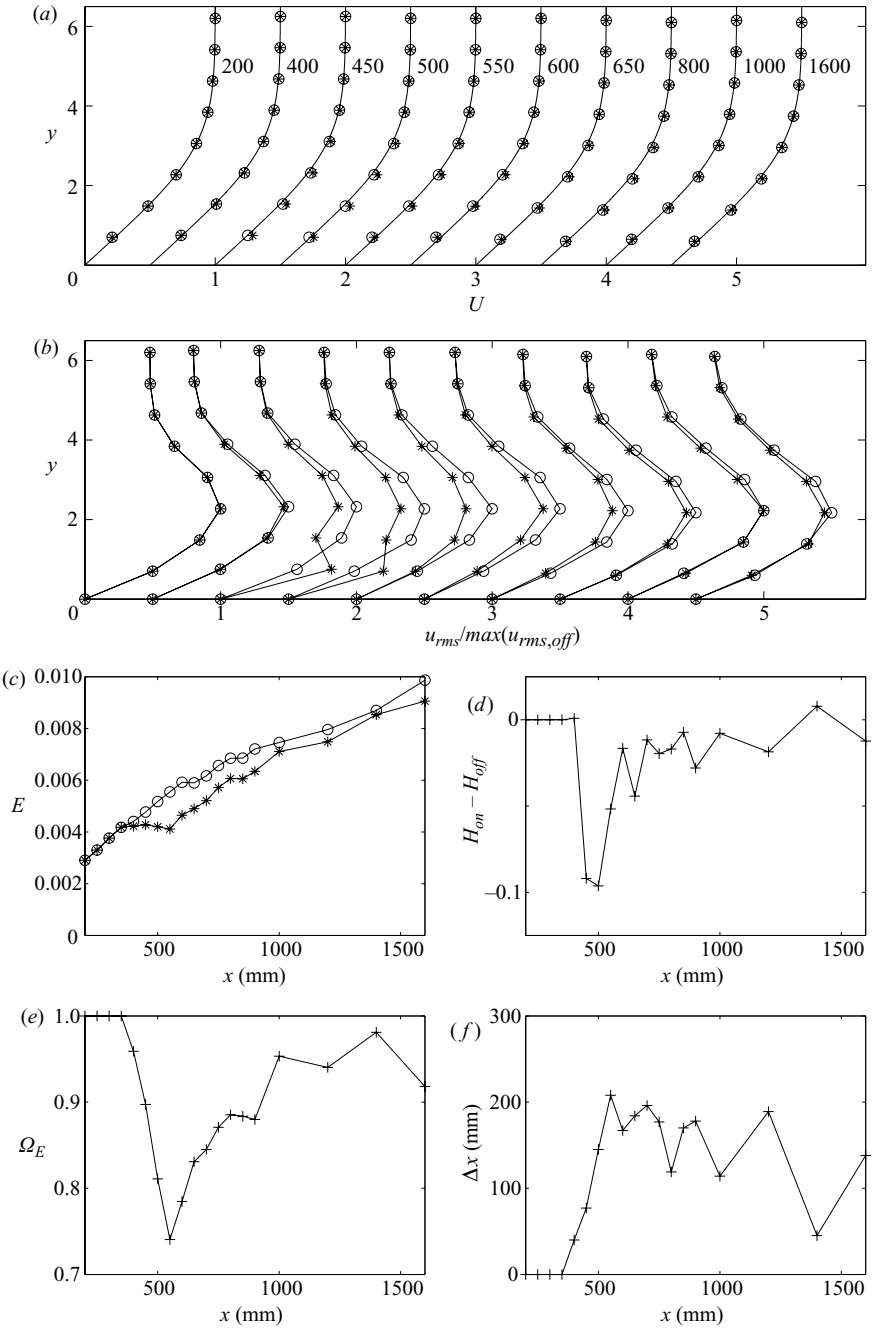

FIGURE 4. Statistics of the mean flow and the disturbance with and without control. (*a*) Mean flow profiles without (○) and with control (∗) at the x-positions indicated next to the profiles, the solid curves show the Blasius profile. (*b*) Profiles of u_{rms} without (○) and with (∗) control at the same x-positions as in (*a*). At each x-position, the profiles are normalized with the maximum value obtained without control. (*c*) Streamwise development of the disturbance energy defined in (3.1) without (○) and with control (∗). (*d*) Difference of the measured value of the shape factor with and without control. (*e*) Streamwise development of the relative disturbance attenuation Ω_E defined in (3.2). (*f*) Streamwise development of Δx defined in (3.4). $Tu = 1.4\,\%$.

The streamwise growth of the disturbance energy in the boundary layer, defined as

$$E(x) = \int_0^6 [u_{rms}(x, y)]^2 \, \mathrm{d}y, \tag{3.1}$$

is shown in figure 4(*d*). The disturbance energy increases from 0.003 at $x = 200$ mm to 0.01 at $x = 1600$ mm. The flow is thus far from transitional in the region under study. Matsubara & Alfredsson (2001) and others report that the disturbance energy grows linearly with x. In the present set-up, the growth is somewhat slower, especially at large x. The reason for this discrepancy from previous studies is probably that Tu is in the lower range and that as it decreases downstream, it does not manage to force the boundary layer as it does at higher levels of Tu. The assumption of the effect of the decaying turbulence is supported by the analysis of Leib *et al.* (1999) and is an indicator of continuous interaction between the fluctuations in the free stream and the flow in the boundary layer.

Integrating the measured disturbance through the boundary layer as in (3.1) requires us to choose an upper bound for the integral, since the disturbance level far from the wall is given by the free-stream turbulence. For cases with a laminar free stream, the disturbance level far from the plate is zero, and the integral can be taken to infinity. Here, $y = 6$ was chosen as a suitable limit. The consistency of E calculated from the sparse data as a measure of the disturbance level was confirmed by measuring the disturbance profile with and without control at $x = 600$ mm and two distributions of the measurement points, one being the standard one (eight points between $y = 0.5$ and $y = 6$) and the other one being 30 points from closer to the wall to $y = 6$. The values of E obtained with the two point distributions differ by only a few per cent.

In the following, we demonstrate the control efficiency, using suitable control parameters given in § 4.4. The influence of the various parameters will be discussed further in § 4. At $x = 200$–350 mm, measurements were performed without control only, since the control did not affect the flow that far upstream of the actuators. At $x = 400$–1600 mm, measurements were performed both with and without control.

The mean velocity profiles with control in figure 4(*a*) show that at $x = 450$ and 500 mm, i.e. just above the control suction hole, there is a deviation between the measurement without control applied as compared with the results with control. The velocity profiles are fuller, and the shear stress consequently higher, when control is applied. The decrease of skin friction thanks to transition delay further downstream must be large enough to compensate for this local increase close to the position of the actuators. At $x > 500$ mm, the effect on the mean velocity profile due to the control is small.

Even though the control has a small effect on the mean flow, the effect on the disturbance growth is substantial. In figure 4(*b*), it can be seen that the control decreases u_{rms} in the centre of the boundary layer from $x = 450$ mm and downstream. At $x = 450$ and 500 mm, there is also an increase closer to the wall. The increase closer to the wall appears because of the actuation and because the hot wire cannot distinguish between streamwise and wall-normal velocity. The fluctuating wall-normal velocity over the control suction hole thus gives an increase in the measured u_{rms}.

The small change of the mean velocity profiles is further illustrated in figure 4(*d*) where the streamwise variation of the change in shape factor is shown. With control applied, the shape factor is seen to decrease about 0.1 at $x = 450$ to $x = 600$ mm. Continuing downstream, the shape factor is not altered significantly by the control.

The control effect can be measured by the relative reduction of the disturbance amplitude. Two definitions will be used, the first is

$$\Omega_E = \frac{E_{on}}{E_{off}}, \tag{3.2}$$

and the second is

$$\Omega_{rms} = \frac{\max[u_{rms,on}(y)]}{\max[u_{rms,off}(y)]}. \tag{3.3}$$

Thus, if $\Omega < 1$ the control reduces the disturbance level in the boundary layer and vice versa. The reason for these multiple definitions is that the parameter variations presented in § 4 were measured only at the point of maximum disturbance level in order to speed up the measurements. The maximum of the fluctuations were usually found around $y = 2.1$, except far downstream for the $Tu = 2.5\,\%$ case, where transition set in and the maximum moved towards the wall (further discussion on this subject can be found in Matsubara & Alfredsson 2001).

In figure 4(*c*), the streamwise development of E is shown with and without control applied. When the control is turned on, the disturbance energy is found to be constant from the control position at $x = 450$ mm and almost 200 mm downstream. Compared to the values without control applied, the maximum energy reduction is found to be 26 % (figure 4*e*). The growth of E downstream of $x = 600$ mm with control applied is probably a combination of disturbances already in the boundary layer entering from the sides, new disturbances being introduced by the free stream and continued growth of the initial disturbances. The second assumption is supported by the asymptotic expansions of Leib *et al.* (1999) and DNS studies of Jacobs & Durbin (2001). The third assumption is consistent with numerical results of Högberg & Henningson (2002), who found that transiently growing disturbances (i.e. initially growing disturbances that are a sum of a number of non-normal decaying modes) are considerably more difficult to control single-mode disturbances. The optimal controller used in the numerical study managed to decrease the amplitude of the transiently growing disturbances over the actuation area but further downstream, the amplitude started to grow again. In this context, it should be mentioned that the results of Lundell & Alfredsson (2003) show that substantial transition delay can be obtained also by moderate reductions of the amplitude of streamwise streaks.

An alternative way to quantify the control effect is to study the distance the disturbance development is delayed by the control, i.e. to determine Δx so that

$$E_{on}(x) = E_{off}(x - \Delta x). \tag{3.4}$$

Figure 4(*f*) shows that Δx reaches a value of approximately 200 mm at $x = 450$ mm and decreases slowly downstream. There is a tendency for Δx to start to decrease downstream of 1000 mm, but the data are too sparse to draw any firm conclusions in this region. Even if the disturbance amplitude starts to grow again downstream of $x = 550$ mm, Δx remains close to constant.

So far, measurements have been presented for positions straight downstream of the control suction hole at $z = 0$ only. In figure 5, the reduction of E owing to the control is shown as a function of z at four streamwise positions. At $x = 500$, 800 and 1000 mm, the measurements have been performed at $-5 < z < 0$ only, whereas at $x = 600$ mm, the measurements are in the range $-10 < z < 5$. At all points, there is a positive control effect. Figure 5 shows that at $x = 500$ mm, only 50 mm downstream of

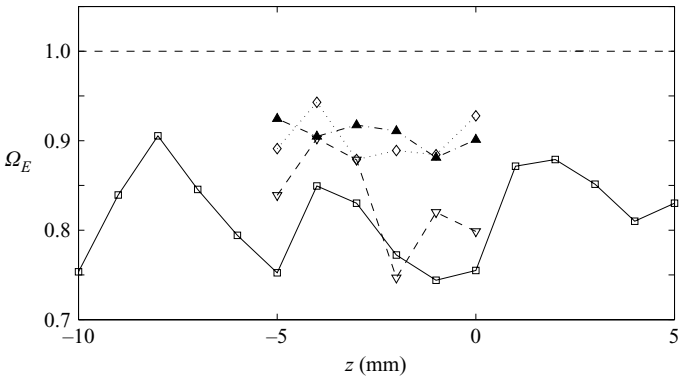

FIGURE 5. Spanwise variation of Ω_E at ▽, $x = 500$; □, 600; ▲, 800 and ◇, 1000 mm as indicated in the label. The dashed line shows 1, the value obtained with no control.

the actuators, there is a strong spanwise variation of the control effect. This is due to the vicinity to the actuation and the mixture of streamwise and wall-normal velocity disturbances detected by the hot wire. Further downstream, at $x = 600$ mm (the solid line), the reduction has a maximum at the spanwise positions of the sensors and control suction holes ($z = -10$, -5, 0 and 5 mm). At these positions, the reduction is around 25 %. In between the control positions, the effect is smaller and the reduction is around 10–15 %. Continuing to $x = 800$ and 1000 mm, the control effect seems to be smeared out in the spanwise direction.

3.2. $Tu = 2.5\,\%$

At $Tu = 2.5$ %, both control units were used and the results are summarized in figure 6. In figure 6(a), the overall growth of the disturbance amplitude is shown both without control and with control unit A applied. The circles show that without control, the disturbance energy grows linearly from $x = 0$ to around $x = 1300$ mm. At this point, a more rapid growth sets in and at $x = 1800$ mm, there is a maximum of the disturbance energy. Further downstream, the amplitude decreases. From previous work (e.g. Matsubara & Alfredsson 2001) it is known that these regions can be attributed to growth of streamwise streaks (first linear part), onset of secondary instabilities (rapid growth) and transition to turbulence (around the point of maximum velocity fluctuations). The point of maximum velocity fluctuations is known to be the point where the intermittency is about 0.5, i.e. the flow is turbulent and laminar half of the time, respectively.

Figure 6(a) also shows the amplitude growth with control applied by control unit A. The triangles show that the control decreases the amplitude somewhat from the actuator position at $x = 450$ mm until the onset of secondary instabilities. The control also results in a slight delay of the onset of the rapid growth, but the effect is minute. This could be expected since the onset of secondary instabilities and creation of turbulent spots means that disturbances spread in the spanwise direction. The streaks, on the other hand, do not spread in the same way.

The efficiency of the two control units in series is shown in figure 6(b–d). Figure 6(b) shows a close up of the energy growth from upstream of the first actuators to just prior to the onset of the rapid growth. The second control unit, whose actuators are positioned at $x = 765$ mm, is seen to decrease the disturbance amplitude further (compare the squares and the triangles). The effect of the second control unit is seen more clearly in figures 6(c) and 6(d), where Ω_E and Δx are shown for three cases:

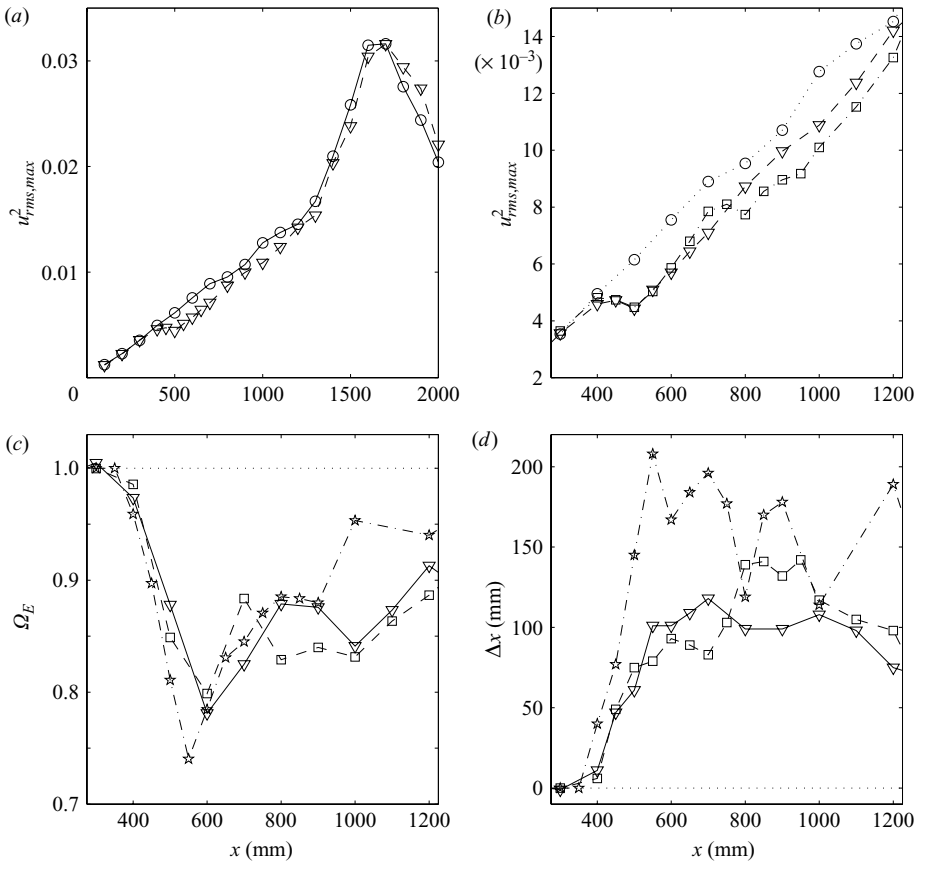

FIGURE 6. Amplitude development with and without control for $Tu = 2.5\,\%$. The symbols are the same in all plots: without control ($\circ$), applying control unit A ($\triangledown$) and applying both control units A and B ($\square$). In (*c*) and (*d*) the values obtained at $Tu = 1.4\,\%$ are shown ($\star$) for comparison. (*a*) Disturbance amplitude as a function of x. (*b*) Close up of the region where the control has the most significant effect. (*c*) Ω_E defined in (3.2) (*d*) Streamwise development of Δx defined in (3.4).

$Tu = 2.5\,\%$ with one (A) and two (A + B) control units applied and $Tu = 1.4\,\%$ with control unit A from figure 4(*c*). The value of Δx is higher at the lower turbulence level, but this effect is somewhat compensated by the second control unit. It is also seen that unit A is considerably more effective than unit B in terms of Δx.

4. Variations of the parameters in the controller

The controller involves three parameters: the delay between detection and actuation, d_c, the flow velocity through the control suction hole, V_w, and finally, the threshold value of the wall shear stress signal below which control suction is turned on, k (which gives the time fraction that suction is turned on, Γ_{on}). These parameters must be tuned to obtain a good control effect. Systematic variations of the parameters in the controller have been performed in order to find suitable values, as well as to explore how sensitive the control effect is with regard to the parameter settings. Typical results for the $Tu = 2.5\,\%$ case, where both control units A and B were used are shown below, followed by the resulting suction times at $Tu = 1.4\,\%$. After this,

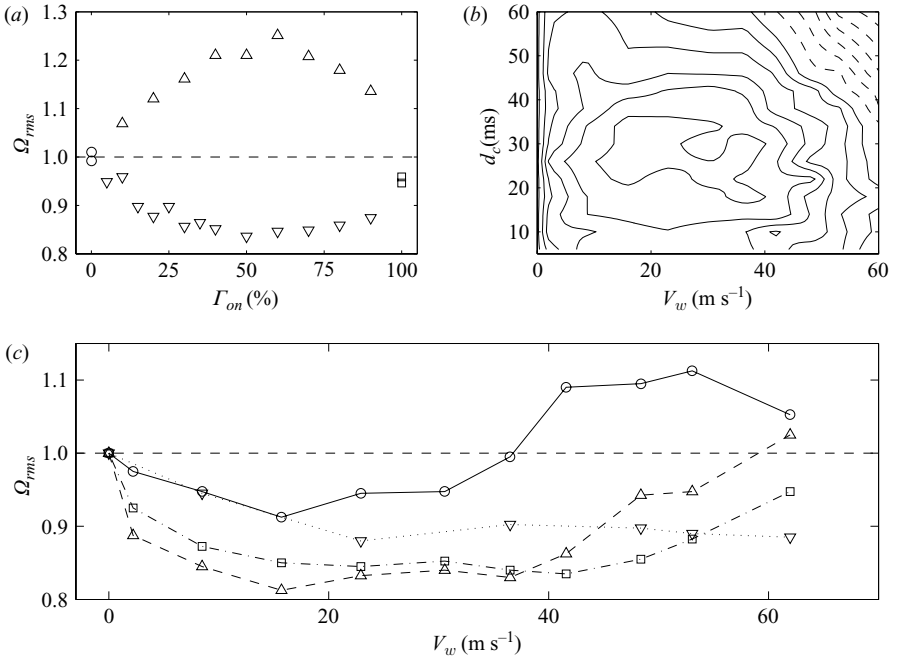

FIGURE 7. Control effect Ω_{rms} for unit A at $x = 600$ mm as a function of (a) the time control suction is applied, (b) the delay in the control loop d_c and the mean suction velocity V_w, and (c) the fraction of time suction is turned on Γ_{on} and V_w. (a) Suction on low velocity ($\triangledown$), suction on high velocity ($\triangle$), no suction ($\bigcirc$), and continuous suction ($\square$). The contours in (b) are separated by 0.03 and positive contours are dashed. (c) Γ_{on} $\bigcirc$, = 100 %; $\triangle$, = 50 %; $\square$, 30 %; $\triangledown$, 10 %.

the parameters chosen for the detailed measurements in the rest of the paper are presented.

4.1. *Control unit A*

4.1.1. *Threshold*

Figure 7(a) shows the control effect at $x = 600$ mm for various threshold values. The control effect is measured as Ω_{rms} defined in (3.3) and the threshold value is not shown explicitly; instead, the resulting fraction of time that control was turned on, Γ_{on}, is shown.

The upwards pointing triangles in figure 7(a) denote suction applied when W is larger than the threshold, whereas the downwards pointing triangles denote suction applied when W drops below the current threshold. Upwards pointing triangles thus denote the result when suction is applied to high-speed streaks while downwards pointing triangles denote suction applied to low-speed streaks.

Studying the downwards pointing triangles in figure 7(a) from $\Gamma_{on} = 0$ % to 100 %, we observe that as suction is applied to regions of negative velocity deviations, the disturbance level is initially decreased. As the threshold value is increased, and suction is applied also to regions of less extreme velocity deviations, the effect flattens out at $\Gamma_{on} = 30$ %, becomes approximately constant until $\Gamma_{on} = 70$ % suction time whereupon the disturbance energy increases towards the continuous suction value. Observe that from $\Gamma_{on} = 50$ % and up, suction is applied also at periods of positive velocity

disturbances. The increase in the disturbance level is thus natural. At $\Gamma_{on} = 100\,\%$, there is only a small control effect remaining.

Finally, attention will be turned to the upwards pointing triangles. They show the response of the flow if suction is applied at instants of high velocity. Doing so, the disturbance level increases, presumably because the amplitude of the high-velocity streaks is enhanced and the low velocity streaks are left as they are. For higher time fractions, suction is applied also to low-speed streaks and the disturbance energy is reduced towards the value obtained at $\Gamma_{on} = 100\,\%$.

4.1.2. *Delay*

The effect of the delay can be deduced from the contours in figure 7(*b*). Following vertical lines, it is found that there is an optimal delay around 30 ms, independent of suction rate. This delay should be compared with the delay that maximizes the correlation between the sensor signal and the velocity signal at the position of control. In the present case, a delay of 46.5 ms maximizes the correlation between the sensor signal at the wall and the velocity at the centre of the boundary layer above the control suction hole. The delay which could be expected from the disturbance velocity, $0.8U_\infty$ (Lundell & Alfredsson 2004), and the distance between sensor and actuator, 236 mm, is 61.5 ms.

There are two main effects which cooperate to give these discrepancies between the optimal (32 ms), the physical (46.5 ms) and the expected delay (61.5 ms). First, Lundell & Alfredsson (2004) showed that the streaks are tilted by the shear so that the upper parts are downstream of the lower parts. Therefore, the centre of a streak is already far downstream of the sensor when it is detected. This explains the difference between the physical and expected delay. There is also a delay (~ 10 ms) from when suction is turned on until full suction is established, which gives the discrepancy between the physical and optimal delay.

It should be noted that the physical delays in the control apparatus and the tilting of the structures together give a minimum feasible distance between the sensor and actuator. Since the structures are growing in length downstream, this minimum distance increases in the downstream direction.

4.1.3. *Suction velocity*

The optimum for the suction velocity in figure 7(*b*) is wide, Ω_{rms} is almost constant from $V_w \approx 10$ to $40\,\mathrm{m\,s^{-1}}$. The effect of suction velocity is also dependent of Γ_{on}, which controls the mean amplitude of the disturbances which are targeted by the control. With a low value of Γ_{on}, it can be assumed that mainly high-amplitude disturbances are targeted, and thus a high suction rate could be feasible. This assumption is confirmed in figure 7(*c*) where the effect of varying the suction velocity at different threshold levels is shown. With continuous suction applied (circles), a small decrease in the disturbance level is seen for low suction velocities while larger suction velocities result in an increase of the velocity fluctuations. The downwards triangles, which initially follow the circles, indicate the disturbance levels obtained when the threshold is set so that suction is applied 10 % of the time (note that this means that the suction volume is 10 % of the continuous suction case). The control is then applied only to the low-velocity streaks which deviate the most from the mean. When applying suction only at the strongest streaks, very high suction velocities still give a reduction in the disturbance amplitude. At $\Gamma_{on} = 10\,\%$, the maximum disturbance reduction is obtained from a suction velocity around $25\,\mathrm{m\,s^{-1}}$.

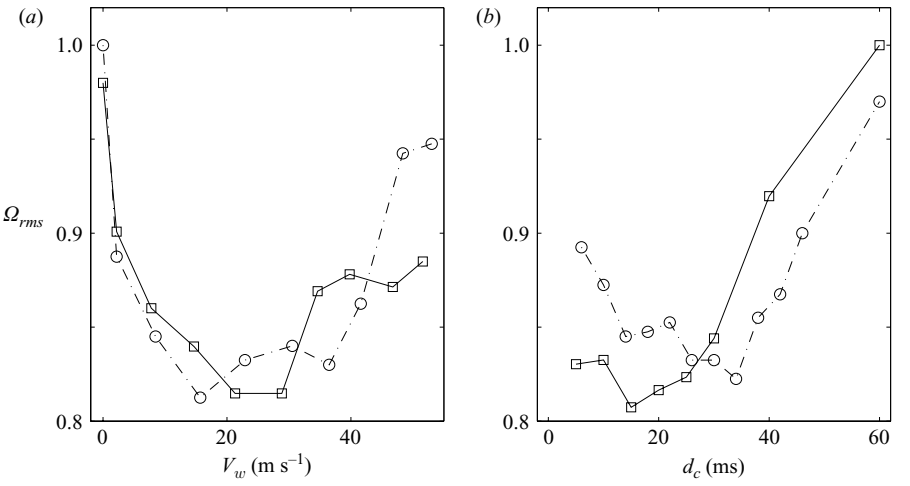

FIGURE 8. Parameter variation for control unit B (□) compared with unit A (○) at $Tu = 2.5\,\%$. (*a*) Effect of suction velocity and (*b*) effect of delay in the control loop.

The squares and upward pointing triangles are the levels obtained when suction is applied 30 % and 50 % of the time, respectively. It is clear that $\Gamma_{on} = 50\,\%$ gives a larger maximum reduction while the control effect remains at higher suction rates for the $\Gamma_{on} = 30\,\%$ case (and even higher suction rates for the 10 % case). The behaviour at high suction rates discussed above is of limited practical interest, since the ultimate goal in, for example, an aerospace implementation would be to minimize the energy expenditure of the system. However, it is important to know the sensitivity to suction which is higher or lower than the selected value since it might be impossible to tune the actuator amplitude at every single position. For the 30 % and 50 % cases, the maximum control effect is obtained around 17 m s^{-1}.

An important conclusion which can be drawn from figure 7(*c*) is that modulated actuation probably has benefits. Since the optimal suction velocity at 10 % is slightly higher than that at 30 % and 50 %, gains can be expected if the suction velocity is varied according to the disturbance amplitude. The data in figure 7 show that automated search algorithms should easily find a desired optimal working point.

4.2. *Control unit B*

The parameter dependence of the downstream control unit, B, is shown and compared with the data for unit A in figure 8. In figure 8(*a*), the optimal value of the suction velocity V_w is seen to be similar for both control units (solid and dashed curves).

The curves in figure 8(*b*) show the control effect for different delays in the control loop d_c. The data reveal that the optimal delay is shorter for unit B than for unit A. This is somewhat surprising, especially since the sensor–actuator distance is 60 % longer in unit B than in unit A. Note that in the present set-up, the distance between sensing and actuation for unit B is 356 mm while for unit A it is only 236 mm. Still, the optimal delay time is significantly lower for unit B.

At first sight, this result might seem to break the simplest logic, but possible mechanisms imposing this effect will be discussed in the following. The control probably has to target the streak where it has its maximum amplitude, i.e. around $y = 2.1$. The physical height is thus increasing as $x^{0.5}$ (see (2.1)), which is why it is

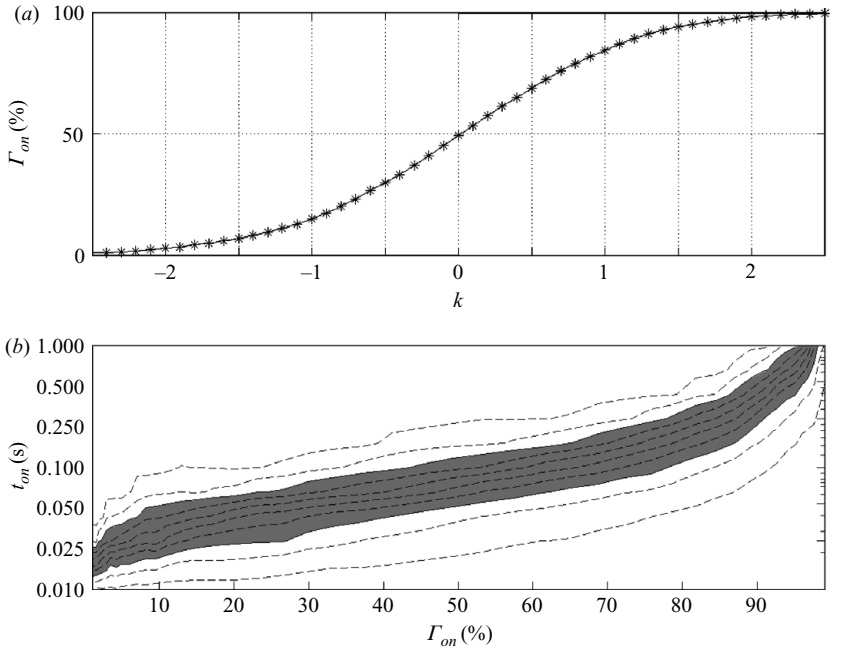

FIGURE 9. (*a*) Relationship between Γ_{on} and k. (*b*) F_{on} defined in (4.2) as a function of Γ_{on} and t_{on}. The contours in (*b*) are 5, 15, ..., 95 % and the region betweeen 25 and 75 % is indicated in grey. $Tu = 1.4\,\%$.

necessary to initialize the control a little more in advance further downstream simply to reach out through the boundary layer in time to cancel the streak. Furthermore, Lundell & Alfredsson (2004) found that the streaks are self-similar not only in the wall-normal coordinate scaled with the boundary-layer thickness, but also in the streamwise coordinate in the same scaling. The streaks are inclined through the boundary layer so that the upper parts are further downstream than their lower parts. The centre of a streak, detected by a sensor, is thus already downstream of the sensor position at the moment of detection because the streak is inclined. The physical distance is increasing downstream since the streak scales with the boundary-layer thickness. This effect can also be seen in the data to be presented in § 5. Consequently, the streak growth in both the streamwise and wall normal direction implies a decrease of the optimal delay time when the control position is moved downstream.

4.3. *Actual suction times*

In order to correlate the somewhat abstract parameter Γ_{on} to the actual wall-wire signals and suction times, figure 9(*a*) shows the relationship between the threshold parameter k and the resulting Γ_{on} for the $Tu = 1.4\,\%$ case. This distribution is given by the temporal behaviour of the wall-wire signal (compare with figure 3).

The time period during which suction is turned on is individual for each event and it is determined by how long the wall-wire signal stays below the threshold. In order to present the distribution of the suction times for different threshold values, the probability density function, $f_{on}(t_{on}, \Gamma_{on})$, of the number of suction periods with

length t_{on}, is introduced and normalized so that:

$$\int_0^\infty f_{on}(t_{on}, \Gamma_{on}) t_{on}\, \mathrm{d}t_{on} = 1. \tag{4.1}$$

The cumulative distribution function of the suction periods can then be introduced as:

$$F_{on}(t_{on}, \Gamma_{on}) = \int_0^{ton} f_{on}(t'_{on}, \Gamma_{on}) t'_{on}\, \mathrm{d}t'_{on}. \tag{4.2}$$

With these definitions, F_{on} is the probability that the suction period is shorter than or equal to t_{on} when suction is applied. Note that the normalization is performed in time rather than per suction event. Many shorter events and one long event are thus given equal weight in the distribution function if they occupy the same total amount of time. Figure 9(*b*) shows contours of F_{on}. The region between 25 and 75 % is grey which means that if the controller is running with a given Γ_{on} and suction is turned on at an instant, the probability is 50 % that the suction period t_{on} will be in the shaded region. The most probable suction period (given by $F_{on} = 50\,\%$) is seen to be short, down to around 0.02 s for low threshold values, and up to 1 s or longer, for high threshold values.

4.4. *Parameter settings during the experiments*

During the control experiments at $Tu = 1.4\,\%$, the threshold was set so that $\Gamma_{on} = 30\,\%$ was obtained. The delay was set to $d_c = 32$ ms and the suction velocity was $28\,\mathrm{m\,s^{-1}}$. At $Tu = 2.5\,\%$, the threshold was chosen to be 0, which gives $\Gamma_{on} = 50\,\%$. The suction velocity was $26\,\mathrm{m\,s^{-1}}$ and the delay was 32 ms for control unit A and 17 ms for unit B.

5. Correlations

With the control effect carefully determined (inhibited growth of the disturbance amplitude from the position of the actuator and 200 mm downstream) and the dependence of the control effect on the parameters in the controller detected, structure development with and without control will be studied. Correlations between the sensors and the hot wire at different positions can be used to study the spatial structure and propagation of the disturbances. The correlation which is presented in this section originates from the $Tu = 1.4\,\%$ case and provides information on how the control affects the streamwise and spanwise sizes of the streaks.

The correlation between the signal from the wall wire at $x = 214$ mm, $z = 0$ and the streamwise velocity variation u at (x, y, z) for a varying delay τ is defined as

$$R_{u,ww}(x, y, z, \tau) = \frac{1}{T} \int_0^T \frac{u(x, y, z, t + \tau)}{u_{rms}} W(t)\, \mathrm{d}t, \tag{5.1}$$

and in the following, different aspects of this correlation will be studied.

5.1. *Streamwise and wall-normal development*

The temporal evolution of the correlation structures are shown in figure 10. Remember that y is non-dimensionalized with the boundary-layer length scale, equation (2.1). The physical boundary layer is 2.8 times as thick at $x = 1600$ mm compared with $x = 200$ mm. At first, the structure is short and as it develops downstream, it grows in length. The length (and height) of the streaks have been found to grow as the boundary-layer thickness, i.e. as $x^{0.5}$ (Matsubara & Alfredsson 2001; Lundell &

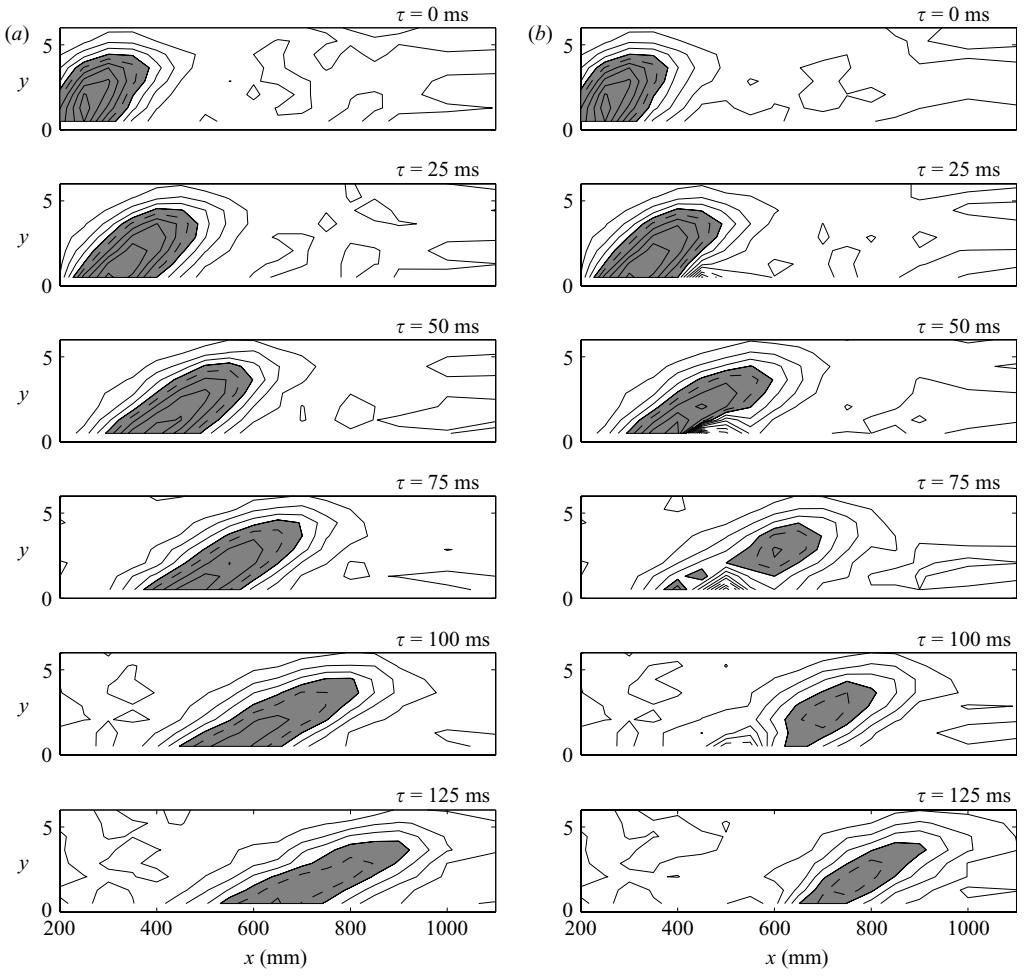

FIGURE 10. Correlation between the wall wire and the hot wire. (*a*) The reference case without control (*b*) with control, and $\tau = 0$–125 ms from top to bottom. Contour separation is 10 %, the 40 % contour is filled with grey and the 50 % contour is dashed. The graphs have to be stretched 10–25 times in the streamwise direction (depending on streamwise position) in order to obtain the physical aspect ratio.

Alfredsson 2004). When control is applied (figure 10*b*), the structures are shorter, especially close to the wall. The correlation between the centre of the boundary layer and the wall is seen to disappear. Note that there is a region of negative correlation around the control suction hole. This is because close to the actuator, there is a region where the fluctuation generated by the actuator (which is negatively correlated with the original disturbance) is stronger than the original disturbance. This effect has severe implications for the possibility of making distributed measurements close to the actuator, measurements which might be necessary if more advanced control algorithms are to be implemented.

In figure 11(*a*), the streamwise development of the maximum correlation (i.e. the value of $R_{u,ww}$ at the delay τ for which $R_{u,ww}$ has its maximum) at the position $(y, z) = (2.1, 0)$ is shown with and without control. The correlation is seen to be close to unity at $x = 250$ mm, i.e. almost straight above the wall wire. Moving the hot wire

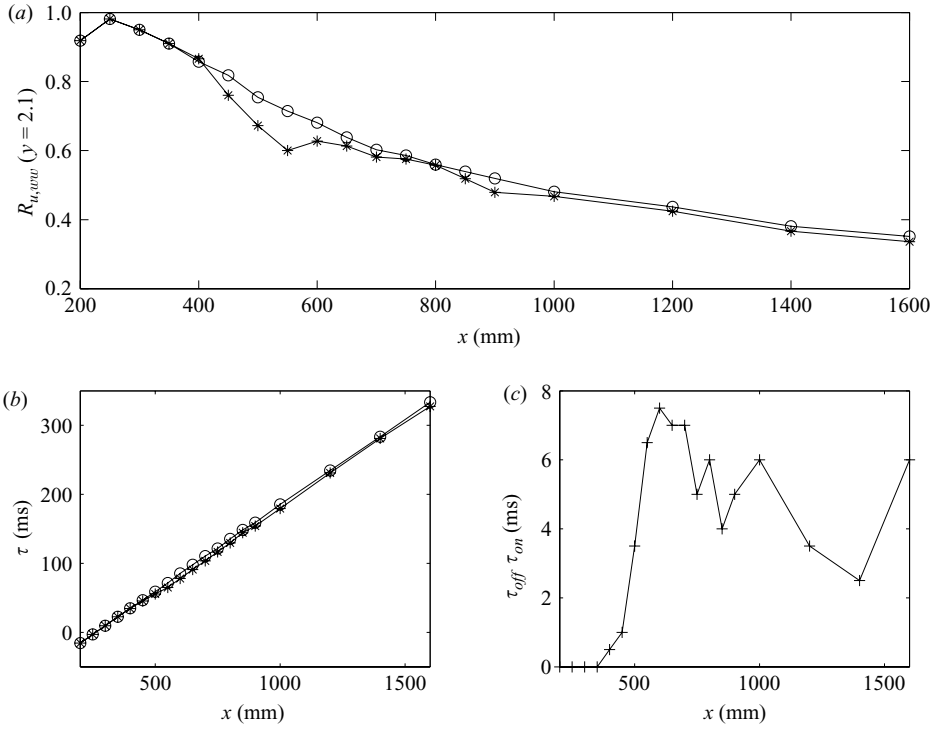

FIGURE 11. Maximum correlation between the wall-wire signal and the velocity measured with the hot wire at $y = 2.1$ in (a) and the delay between the signals at which this correlation is obtained (b) without (○) and with control (∗). In (c), the difference of the delay with control on and off is shown.

downstream, the correlation decreases. At the streamwise position of the actuator, $x = 450$ mm, the correlation has dropped to just above 0.80. Further downstream, the correlation continues to decrease and becomes 0.35 at $x = 1600$ mm. With control applied, the correlation is slightly decreased in the region where the growth of disturbance amplitude is inhibited ($x = 450$ to 600 mm). Apart from this region, the control does not have a large effect on the correlation between signals from the wall wire and the hot wire.

Effects due to the control are also found in the delays maximizing the correlation, τ_{max}, which are shown in figure 11(b) (not to be confused with the delay d_c used in the controller). Without control, τ_{max} grows linearly in the downstream direction, a result indicating that the structures in the boundary layer propagate downstream with constant velocity (note that the tilting of the structures gives a negative τ at $x = 250$ mm, i.e. the streaks reach the hot wire, placed downstream of the wall wire at $x = 214$ mm, before they are detected by the wall wire. The effect due to the control is not large in figure 11(b), even though it can be seen that the delay becomes somewhat lower from $x = 450$ mm and downstream with control applied. The difference is accentuated in figure 11(c), where the difference in delay, $\tau_{max,off} - \tau_{max,on}$ with and without control applied is plotted. The delay is found to be up to 8 ms shorter when control is applied. This means that with control applied, the disturbances correlated with the wall-wire signal appear 8 ms earlier at $x = 600$ mm as compared with the case without control applied.

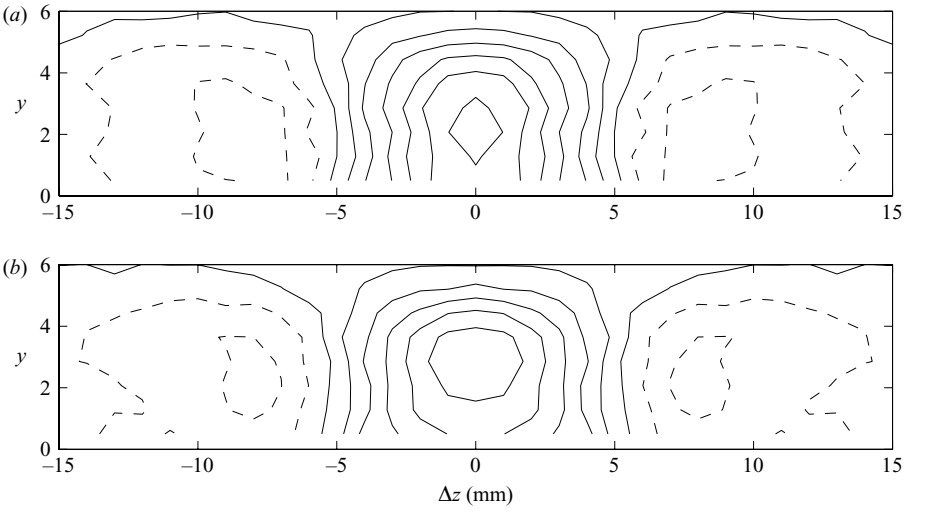

FIGURE 12. Cross-flow distribution of the maximum correlation between the wall wire at $x = 214$ mm and the velocity at $x = 600$ mm, $y = 2.1$ with separation Δz between the wall wire and the hot wire (*a*) without and (*b*) with control applied. Contour spacing is 10 % and negative contours are dashed. The correlation has been calculated for positive separations, averaged over the four wall wires, and is mirrored around $\Delta z = 0$.

In figure 10, the correlation between the disturbance at the sensing position, $x = 214$ mm, is found to have a correlation of 80 % with the disturbances at the actuation position, $x = 450$ mm. By applying linear system identification (e.g. Wiener filters as used by Amonlirdviman & Breuer 2000) it is possible to increase this value to 82–83 %. The benefit from using linear system identification is thus very small in the present case, and was not further pursued.

An important consequence of figure 10(*b*), which must be taken into account when designing control systems with more densely distributed sensors, is that the information obtainable at the wall just downstream of the control does not reflect the developments in the flow above, owing to the strong localized actuation. This problem might be less severe with distributed low-amplitude actuation.

5.2. *Spanwise structure*

The cross-stream structure of the disturbances is illustrated in figure 12. The maximum correlation between the wall-wire sensor and the hot wire at $x = 600$ mm is shown. To obtain the correlation for different Δz, the hot wire was traversed in between two of the wall wires, whereupon the correlations were calculated between the hot-wire signal and the signal from suitable wall wires. In order to increase the visual impact of the data, the data has been mirrored around $\Delta z = 0$. The effects of the control on the cross-stream distribution are small. Neither the spanwise width nor the height of the structures are affected by the control. The only noteworthy difference is that without control in figure 12(*a*), the structure extends all the way down to the wall, whereas with control applied, the correlation is lower close to the wall. The cross-stream structure is very similar at different streamwise positions (except for the maximum value which decreases as shown in figure 11) but are not shown.

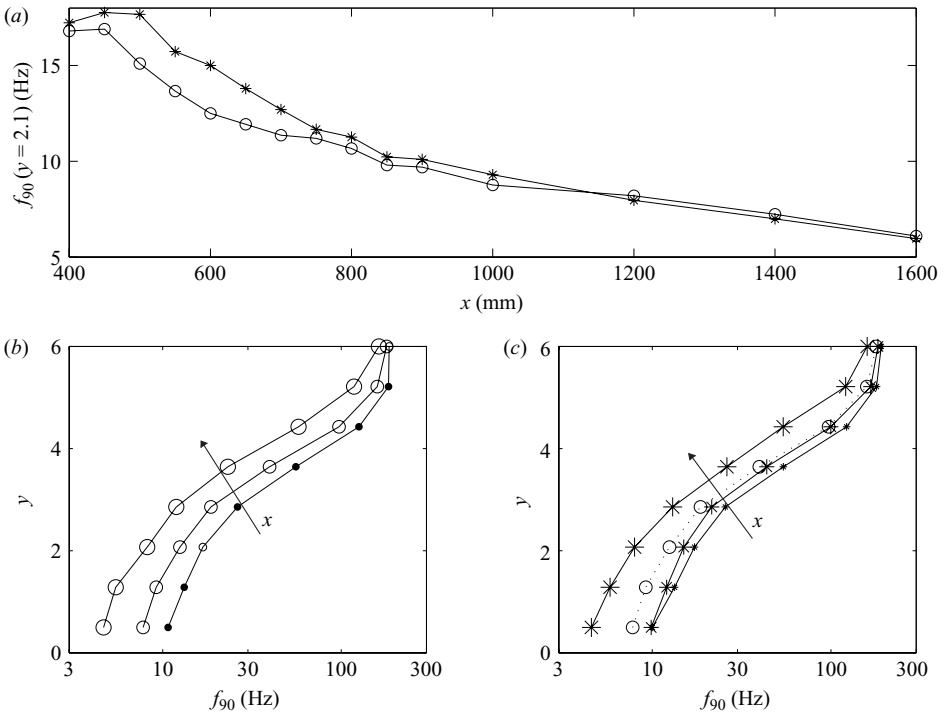

FIGURE 13. Some aspects of the frequency below which 90 % of the disturbance energy appears, f_{90}; (*a*) streamwise development of f_{90} at $y = 2.1$ without (○) and with control (∗), (*b*) wall normal variation of f_{90} at $x = 400$, 600 and 1200 mm (increasing with marker size) without control and (*c*) wall normal variation of f_{90} at $x = 400$, 600 and 1200 mm (increasing with marker size) with control. In (*c*), the values obtained at $x = 600$ mm without control have been included to facilitate comparison.

6. Spectra

In order to illustrate the variation of the spectral content of the velocity signals, a quantity denoted by f_{90} will be used. The definition of f_{90} is such that 90 % of the spectral energy appears at frequencies lower than f_{90}.

6.1. *Streamwise development*

As mentioned, Matsubara & Alfredsson (2001) and Lundell & Alfredsson (2004) reported that the streamwise length scale increases with the boundary-layer thickness. This was first concluded because the spectra for low frequencies could be made to collapse if the frequency was non-dimensionalized with the boundary-layer thickness and the free-stream velocity, and then verified by correlation measurements. In terms of f_{90}, this implies a decrease in the streamwise direction.

In figure 13(*a*), f_{90} is shown for various x with and without control. Without control (○), the value decreases from 16 Hz at $x = 400$ mm to just below 6 Hz at $x = 1600$ mm. When control is applied, f_{90} is almost constant from $x = 400$ to 600 mm, the region in which fluctuation growth is inhibited by the control. After $x = 600$ mm, the values with control approach the values obtained without control. As opposed to the disturbance energy, the frequency is returning to the uncontrolled values at $x = 1200$ mm. The frequency is not delayed a certain distance, instead it is constant for some distance

downstream of the control. Further downstream no difference between the two cases can be detected.

6.2. *Wall-normal structure*

Without control, figure 13(*b*), the boundary layer is seen to filter out the high frequencies from the free stream and amplify the low ones, in general agreement with the conclusions of Leib *et al.* (1999) and Ricco *et al.* (2004). There is a monotonous decrease towards the wall from $y = 6$, where f_{90} is around 170 Hz at all streamwise positions, down to the wall where the minimum value of f_{90} is reached at the most downstream position and reads around 8 Hz. The curves from the three streamwise positions appear side by side.

Comparing figures 13(*b*) and 13(*c*) (in (*c*), the values without control at $x = 600$ mm are shown with dots), it is seen that the control mainly decreases the low-frequency fluctuations close to the wall. With control applied (figure 13*c*), the curves for $x = 400$ and 600 mm collapse close to the wall. Further out towards the free stream, the behaviour with and without control is more similar. These results confirm and quantify the results from figure 10, namely that the control inhibits the elongation (trend towards lower frequencies) of the disturbances in the lower part of the boundary layer.

7. Discussion

Control of velocity streaks, generated by a turbulent free stream in a laminar boundary-layer, has been studied. Compared to the previous studies, the present experiment allows a detailed study of the control effect. Not only has the disturbance amplitude have been measured, but detailed studies of the disturbance structure with and without control have been made. The threshold-and-delay control algorithm used in the present experiments makes the control logic simple, easily tunable and scalable. The main result, i.e. that the disturbance amplitude development is delayed 50–200 mm per control unit, is clear in figures 4(*f*) and 6(*d*). The longest delay is achieved at the low *Tu*-level and the shortest for the downstream control unit at the high level.

The results from the variation of the threshold in figure 7(*a*) serve as a good illustration of the most important differences of the present work when compared with two of the previous experimental studies on reactive flow control, namely Rathnasingham & Breuer (2003) and Kerho *et al.* (2000).

In Rathnasingham & Breuer (2003), reactive control was applied to a turbulent boundary layer and the bursting frequency, pressure fluctuations and friction drag, measured from the mean velocity profiles, were decreased. However, their actuator could produce actuation with one sign only, while their controller resulted in control signals of both signs. In the present set-up, this would correspond to applying suction to both high- and low-speed streaks, which of course would reduce the positive effect of the control (or actually cancel it completely). Nevertheless, the results of Rathnasingham & Breuer (2003) are important since they illustrate that linear cancellation achieved by FIR-filters can control turbulence. Whether the performance of such a controller (which is doomed to be complicated from a technical perspective owing to the modulated actuation) is considerably better than what can be achieved with simple controllers such as the one used in the present study, is an open question.

Kerho *et al.* (2000) used reactively controlled intermittent suction to decrease the drag in a turbulent boundary layer and they report a considerable control effect

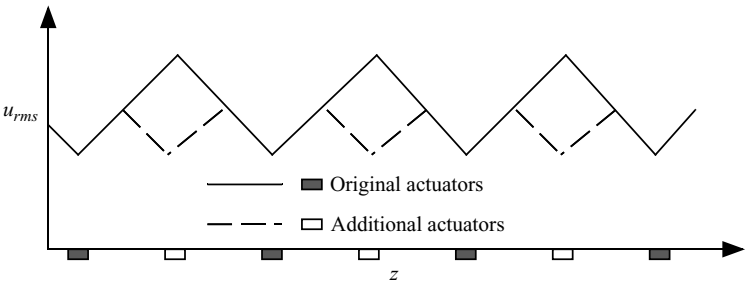

FIGURE 14. Schematic of spanwise disturbance distribution with increased numbers of sensors and actuators.

for continuous suction, as opposed to the present study. In the case of Kerho *et al.* (2000), the control effect was only slightly increased for reactively controlled suction, as compared with continuous suction through the same suction ports. In the present study, we show that all the control is due to the reactively controlled suction, which gives an even higher reduction in energy used for maintaining the suction.

If the flow rate used during the control experiments, q, through one of the control holes is averaged over the area, A, where the control has an effect, 5 mm $\times$ 200 mm (i.e. the actuator separation multiplied by the disturbance development delay, Δx) and is corrected for the time that suction is turned on, the suction coefficient defined by $C_q = \Gamma_{on} q / U_\infty A$ becomes 1.7×10^{-4}. This is around 1 % of $U_\infty \delta_{99} \Delta z$ where δ_{99} is the boundary-layer thickness and Δz is the spanwise spacing of the sensors.

This suction coefficient is almost equal to the suction coefficient necessary to delay breakdown of streaks in a plane channel flow as studied by Lundell & Alfredsson (2003). It is approximately one sixth of the uniform suction necessary to inhibit disturbance growth in a boundary layer subjected to similar levels of FST (Yoshioka, Fransson & Alfredsson 2004). Reactive control can thus decrease the necessary suction volumes compared with continuous distributed suction. The energy spent on maintaining the suction is, however, much larger in the present case, since the localized suction gives rise to very high suction velocities. The physical mechanisms differ in the two cases: in the present case, the actual structures are targeted while continuous suction relies on stabilizing the mean flow profile.

From figure 5, showing the spanwise distribution of disturbance energy, it can be conjectured that increasing the sensor and actuator density by a factor of two can improve the spanwise control result substantially (cf. figure 14). Allowing some speculation, the spanwise profile at $x = 600$ mm (figure 5) would then have a maximum around 0.82 rather than 0.92 as it is now. Consequently, the level at which the fluctuation energy is smeared out further downstream should also be reduced. Increasing the sensor/actuator density even further will probably give smaller gains in the disturbance attenuation. The physical reason for this might be that with double the present density, most (low-speed) streaks can be reduced. In the present experiment, the sensor separation is just large enough for a streak to pass in between two sensors without detection. In this context it should also be noted that Lundell & Alfredsson (2003) showed that in order to delay transition of streaks in a channel flow with localized suction, the suction must be applied within a narrow region around the centre of the streaks.

If doubling the actuator density, the actuator separation would be approximately 20–23 ℓ^+ for units A and B. The resulting actuator separation, 2.5 mm, is

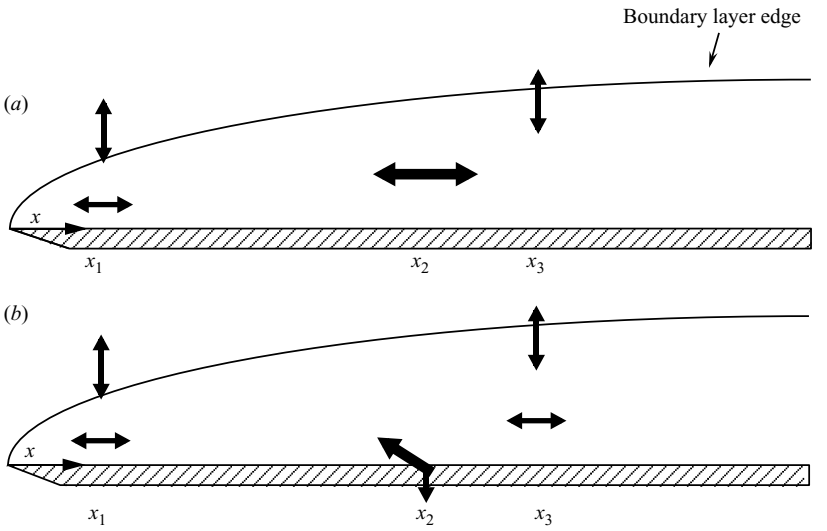

FIGURE 15. Illustration of the attempt to explain the decrease in delay maximizing the correlation due to the control. (*a*) Without control. (*b*) With control.

approximately a third of the streak spacing deduced from the correlation data in figure 12. Alfredsson & Matsubara (2000) noted that the streak width scaled with the friction length is a critical measure in subcritical transition scenarios such as the present one. With this observation in mind, it is not clear that the necessary actuator separation scales with $\delta \sim x^{0.5}$, it is possible that $\ell^+ \sim x^{0.25}$ is the correct scaling. It is important to know the scalings in order to be able to approximate the number of sensors and actuators necessary in engineering applications.

Finally, the change of the delay time maximizing the correlation in figure 11 will be discussed. It was noted that with control, the maximum correlation between the wall-wire signal and the velocity in the boundary layer occurred up to 8 ms earlier as compared with the case without control. The physical interpretation of this is that the disturbances reach downstream positions faster when control is applied.

One possible explanation of this effect would be that the structures accelerate owing to the control and thereby reach the positions downstream of the control earlier. The structures would have to increase their velocity at the control position and gain 8 ms from $x = 450$ mm (the control position) to $x = 550$ mm (see figure 11*c*). After this initial and quick acceleration at $x = 450$ mm, the structures would have to decelerate at $x = 550$ mm and move with the same velocity as without control applied. Such a behaviour seems unlikely and an alternative mechanism will be proposed below.

A possible scenario will be given based on the sketch in figure 15. Consider the boundary layer over the flat plate, subject to disturbances in the free stream. Initially, a disturbance in the free stream (illustrated by the vertical arrow) introduces a small-amplitude streak (the horizontal arrow) in the boundary layer at x_1. The streak is growing in amplitude and length while propagating downstream with a velocity around $0.8U_\infty$ (Lundell & Alfredsson 2004), whereas the free-stream disturbance is convected with the velocity U_∞. When the streak has moved to x_2, the faster free-stream disturbance has reached x_3, as indicated in figure 15. The velocity signal at x_2 will of course be correlated to the wall-shear disturbance detected at x_1 with

a proper time delay between the signals. A moment later, the streak will reach x_3, giving a correlation between the velocity at this position and the shear stress at x_1.

When control is applied, the situation becomes somewhat different. Assuming that the control suction, positioned at x_2, completely removes the streak introduced at x_1 (not by forcing it into the wall as indicated in figure 15, but by rearranging the momentum in the boundary layer), the main contribution to the correlation between the shear stress at x_1 and the velocity at x_3 could be a new, weak but growing, streak, generated by the free-stream disturbance downstream of x_2 and thereby not influenced by the control. Possible mechanisms for such 'streak regeneration' are provided by the asymptotic expansion theories (Wundrow & Goldstein 2001) as well as DNS studies (Jacobs & Durbin 2001). At x_3, the new streak has not yet grown to high amplitudes, but with the control suction removing the streak generated upstream, it may give a considerable contribution to the correlation between the signals. This correlation will of course be obtained with a shorter delay between the signals as compared with the case without control applied since the generating disturbance in the free stream is faster than the disturbances in the boundary layer. Once created, the streak created at x_3 will propagate with the typical structure velocity.

Assume that the disturbance at x_1 is created at $t = 0$ and that x_1 is somewhere close to the leading edge, e.g. at $x = 100$ mm. Without control, the streak will arrive at x_3 (which we assume to be at $x = 500$ mm) at $t_{off} = 0.8U_\infty/(x_3 - x_1)$. Inserting the numbers we obtain $t_{off} = 100$ ms. For the case with control, the new streak created at x_3 will appear at $t_{on} = U_\infty/(x_3 - x_1)$, giving $t_{on} = 80$ ms. The difference is thus 20 ms. The observed value is 7–8 ms, which seems plausible since the effect of the control on disturbance energy was around 25 %.

The physical situation differs from the discussion above so that in the real situation there is a continuous forcing on the boundary layer from the free stream. The disturbances observed at a specific x are thus the integrated result of the continuous forcing and the amplification of disturbances by the boundary layer. To fully understand the mechanism behind the early arrival with control applied, a better understanding of the fundamental physics of how disturbances in the free stream force streaks in the boundary layer is needed.

The near-constant correlation with and without control (see figure 11*a*) together with the change in arrival time indicate that at least some of the energy appearing downstream of $x = 600$ mm (figure 4*d*) with control applied is due to new streaks created by disturbances in the free stream. The reasoning behind this assumption is that streaks entering from the sides would not be correlated with the wall wire. Therefore, the downstream correlation should decrease with control applied if such streaks were the source of the disturbance growth downstream of the control.

8. Conclusions

A reactive control system has been used to control disturbances in a boundary layer subjected to free-stream turbulence. Wall wires were used to sense disturbances in the boundary layer and further downstream, suction through narrow holes were used to decrease the amplitude of structures of low velocity passing over the hole. A parameter variation was performed in order to find the optimal working conditions of the controller.

The effects of the control are summarized below.

(i) Applying the control did not change the mean flow, except very close to the control suction hole, where the velocity profile became fuller.

(ii) The growth of the amplitude of the streamwise velocity fluctuations were inhibited from the actuation position and up to 200 mm downstream, corresponding to approximately 40 boundary-layer thicknesses.

(iii) The control effect is a well-behaved function of the parameters in the controller.

(iv) The optimal delay time between sensing and actuation decreases downstream.

(v) The correlation between the sensor and the velocity decreased in a narrow neighbourhood of the control hole only.

(vi) The maximum correlation between the upstream wall wire and the downstream hot wire occurred at shorter delays with control applied, i.e. the structures appeared earlier with control applied.

(vii) The spanwise structure of the disturbances seemed not to be changed by the control.

(viii) The streamwise development of the spectra towards lower frequencies were inhibited in the region in which the disturbance amplification is inhibited.

Based on these facts, it was concluded that the amplitude of the low-velocity streaks is decreased by the control, giving the decrease in energy growth. The growth of disturbance energy appearing downstream of the controlled region could be explained with an analogy to the results of Högberg & Henningson (2002), who found that optimal disturbances in a spatially developing boundary layer start growing again downstream of the region in which the disturbances are controlled. The mechanism might also be streaks entering from the sides or new streaks being generated by the free stream. It was argued that the latter effect is consistent with the observed decrease of the delay maximizing the correlation between the sensor and velocity signals.

If the growth is due to disturbances entering from the sides, actuators at one streamwise position might be enough to delay transition. If, however, new streaks are created by the free stream, or by the disturbances remaining after the control, spanwise rows of actuators and sensors must be placed after each other in the streamwise direction. A problem which then arises is that downstream of an actuator, the state of the flow in the boundary layer cannot be detected at the wall, since the suction through the hole destroys the correlation between the shear stress at the wall and flow in the boundary layer. In the present experiments, this was overcome to some extent by off-setting the sensors of control units A and B in the spanwise direction. With increasing sensor and actuator density, this solution might not be possible and careful placing of the sensors and actuators would be necessary for the sensors to provide as much information of the flow as possible.

From the parameter study, it was found that high-speed streaks were amplified by the suction while the amplitude of low-speed streaks was decreased. The optimal delay time in the controller decreased downstream. This may be explained by the increase of both streak length and boundary-layer height. This effect gives a fundamental (lower) limit on sensor–actuator distance which has to be taken into account when designing control systems to be applied in various applications.

The spanwise disturbance distributions indicate that the control effect would be almost uniform in the spanwise direction if the actuator spacing is half the spacing used in the present experiment. This means that an actuator spacing of $25\ell^+$ or 2δ is

required to control streaks such as the present ones. The resulting spacing, 2.5 mm, is about one-third of the streak spacing found by spanwise correlation measurements.

The present experiment shows that substantial control effects can be obtained with simple control logic, which is easily scalable. The parameters of the controller are easily tuned to desired optima and the control effect is robust with respect to slight variations of the parameters. In order for the results to have practical importance, the actuator technology requires substantial development. If only robust and durable wall-mounted actuators were available, large-scale tests closer to conditions found in applications could be made. To design and fabricate such actuators that are easily maintained and have small energy expenditure at sufficiently low cost is a challenging engineering task.

Future studies should aim at establishing how the physical actuators can be modelled and whether it is the actuator technology or controller algorithms, or both, which present the impressive results from numerical studies from being reproduced in the laboratory. The fundamental design constraints, such as the minimum streamwise sensor–actuator distance and the relative positioning of sensors and actuators, also leave a number of open questions which are critical for the design of efficient control systems.

This work has relied on the scientific guidance of and been inspired by Professor P. Henrik Alfredsson. The craftsmanship of Marcus Gällstedt and Ulf Landén has been indispensable during the designing and building of the set-up. This work has been partly financed by the Swedish Research Council

REFERENCES

Alfredsson, P. H. & Matsubara, M. 2000 Free-stream turbulence, streaky structures and transition in boundary layer flows. *AIAA Paper* 2000-2534.

Amonlirdviman, K. & Breuer, K. S. 2000 Linear predictive filtering in a numerically simulated turbulent flow. *Phys. Fluids* **12**, 3221–3228.

Andersson, P., Berggren, M. & Henningson, D. S. 1999 Optimal disturbances and bypass transition in boundary layers. *Phys. Fluids* **11**, 134–150.

Andersson, P., Brandt, L. & Henningson, D. S. 2001 On the breakdown of boundary layer streaks. *J. Fluid Mech.* **428**, 29–60.

Asai, M., Minagawa, M. & Nishioka, M. 2002 The instability and breakdown of a near-wall low-speed streak. *J. Fluid Mech.* **455**, 289–314.

Bakchinov, A. A., Grek, G. R., Klingmann, B. G. B. & Kozlov, V. V. 1995 Transition experiments in a boundary layer with embedded streamwise vortices. *Phys. Fluids* **7**, 820–832.

Bakchinov, A. A., Katasonov, M. M., Alfredsson, P. H. & Kozlov, V. V. 1999 Control of boundary layer transition at high FST by localized suction. In *IUTAM Symp. on Mechanics of Passive and Active Flow Control* (ed. G. E. A. Meier & P. R. Viswanath), pp. 159–164. Kluwer.

Bewley, T. R., Moin, P. & Temam, R. 2001 DNS-based predictive control of turbulence: an optimal benchmark for feedback algorithms. *J. Fluid Mech.* **447**, 179–225.

Chang, Y., Collis, S. S. & Ramakrishnan, S. 2002 Viscous effect in control of near-wall turbulence. *Phys. Fluids* **14**, 4069–4080.

Choi, H., Moin, P. & Kim, J. 1994 Active turbulence control for drag reduction in wall-bounded flows. *J. Fluid Mech.* **262**, 75–110.

Elofsson, P. A., Kawakami, M. & Alfredsson, P. H. 1999 Experiments on the stability of streamwise streaks in plane Poiseuille flow. *Phys. Fluids* **11**, 915–930.

Endo, T., Kasagi, N. & Suzuki, Y. 2000 Feedback control of wall turbulence with wall deformation. *Intl J. Heat Fluid Flow* **21**, 568–575.

Fasel, H. F. 2002 Numerical investigation of the interaction of the Klebanoff-mode with a Tollmien–Schlichting wave. *J. Fluid Mech.* **450**, 1–33.

Fransson, J. H. M. & Alfredsson, P. H. 2003 On the disturbance growth in an asymptotic suction boundary layer. *J. Fluid Mech.* **482**, 51–90.

Gad-el-Hak, M. 1989 Flow control. *Appl. Mech. Rev.* **42**, 261–292.

Hamilton, J. M., Kim, J. & Waleffe, F. 1995 Regeneration mechanisms of near-wall turbulence structures. *J. Fluid Mech.* **287**, 317–348.

Hœppner, J., Brandt, L. & Henningson, D. S. 2005 Transient growth on boundary layer streaks. *J. Fluid Mech.* **537**, 91–100.

Högberg, M. & Henningson, D. S. 2002 Linear optimal control applied to instabilities in spatially developing boundary layers. *J. Fluid Mech.* **470**, 151–179.

Inasawa, A., Lundell, F., Matsubara, M., Kohama, Y. & Alfredsson, P. H. 2003 Velocity statistics and flow structures observed in bypass transition using stereo PTV. *Exps. Fluids* **34**, 242–252.

Jacobs, R. G. & Durbin, P. A. 2001 Simulations of bypass transition. *J. Fluid Mech.* **428**, 185–212.

Jacobson, S. A. & Reynolds, W. C. 1998 Active control of streamwise vortices and streaks in boundary layers. *J. Fluid Mech.* **360**, 179–211.

Jonáš, P., Mazur, O. & Uruba, V. 2000 On the receptivity of the by-pass transition to the length scale of the outer stream turbulence. *Eur. J. Mech.* B/*Fluids* **19**, 707–722.

Kendall, J. M. 1998 Experiments on boundary-layer receptivity to freestream turbulence. *AIAA Paper* 98-0530.

Kerho, M., Heid, J., Kramer, B. & Ng, T. 2000 Active drag reduction using selective low rate suction. *AIAA Paper* 2000-4018.

Klingmann, B. G. B., Boiko, A., Westin, K. J. A., Kozlov, V. V. & Alfredsson, P. H. 1993 Experiments on the stability of Tollmien–Schlichting waves. *Eur. J. Mech.* B/*Fluids* **12**, 493–514.

Landahl, M. T. 1980 A note on an algebraic instability of inviscid shear flows. *J. Fluid Mech.* **98**, 243–251.

Leib, S. J., Wundrow, D. W. & Goldstein, M. E. 1999 Effect of free-stream turbulence and other vortical disturbances on a laminar boundary layer. *J. Fluid Mech.* **380**, 169–203.

Lindgren, B. 2003 Flow facility design and experimental studies of wall-bounded turbulent shear-flows. PhD thesis, Royal Institute of Technology, TRITA-MEK 2002:16.

Luchini, P. 2000 Reynolds number independent instability of the boundary layer over a flat surface: optimal perturbations. *J. Fluid Mech.* **404**, 289–309.

Lumley, J.L. 1970 *Stochastic TOols in Turbulence*. Academic.

Lundell, F. & Alfredsson, P. H. 2003 Experiments on control of streamwise streaks. *Eur. J. Mech.* B/*Fluids* **22**, 279–290.

Lundell, F. & Alfredsson, P. H. 2004 Streamwise scaling of streaks in a boundary layers subjected to free-stream turbulence. *Phys. Fluids* **14**, 1814–1817.

Matsubara, M. & Alfredsson, P. H. 2001 Disturbance growth in boundary layers subjected to free stream turbulence. *J. Fluid Mech.* **430**, 149–168.

Rathnasingham, R. & Breuer, K. S. 2003 Active control of turbulent boundary layers. *J. Fluid Mech.* **495**, 209–233.

Rebbeck, H. & Choi, K.-S. 2001 Opposition control of near wall turbulence with a piston-type actuator. *Phys. Fluids* **13**, 2142–2145.

Reddy, S. C., Schmid, P. J., Baggett, J. S. & Henningson, D. S. 1998 On stabililty of streamwise streaks and transition thresholds in plane channel flows. *J. Fluid Mech.* **365**, 269–303.

Ricco, P., Durbin, P. A., Zaki, T. & Wu, X. 2004 Nonlinear evolution of velocity fluctuations in a laminar boundary layer excited by free-stream vortical disturbances. In *Proc. Summer Program 2004*, pp. 223–240. Centre for Turbulence Research.

Sahlin, A., Johansson, A. V. & Alfredsson, P. H. 1988 The possibility of drag reduction by outer layer manipulators in turbulent boundary layers. *Phys. Fluids* **31**, 2814–2820.

Waleffe, F. 1995 Hydrodynamic stability and turbulence: beyond transients to a self-sustained process. *Stud. Appl. Maths* **95**, 319–343.

Wundrow, D. W. & Goldstein, M. E. 2001 Effect on a laminar boundary layer of small-amplitude streamwise vorticity in the upstream flow. *J. Fluid Mech.* **426**, 229–262.

Yoshioka, S., Fransson, J. H. M & Alfredsson, P. H. 2004 Free stream turbulence induced disturbances in boundary layers with wall suction. *Phys. Fluids* **16**, 3530–3539.

Zaki, T. A. & Durbin, P. A. 2006 Mode interaction and the bypass route to transition. *J. Fluid Mech.* **531**, 85–111.